Breast-Cancer Tumor Localization and Sizing by Functional Diffuse Optical Tomographic Imaging Combined with Controlled Compression Protocols

Randall L. Barbour[1,2], Rabah M. Al abdi[3], Yong Xu[1,2], and Harry L. Graber[1,2]
[1]*SUNY Downstate Medical Center,450 Clarkson Ave, Brooklyn NY 11203*
[2]*NIRx Medical Technologies LLC, 15 Cherry Lane, Glen Head NY 11545, USA*
[3]*Jordan University of Science and Technology, Irbid 22110, Jordan*
randall.barbour@downstate.edu

Abstract. Optical breast imaging studies show that controlled pressure maneuvers improve contrast between tumors and both the surrounding healthy tissue and the contralateral breast. The accuracy of tumor localization and sizing was consequently improved.
OCIS codes: (170.3830) Mammography; (170.2655) Functional monitoring and imaging; (120.5475) Pressure measurement

1. Introduction

Details of blood delivery to tissue, and of bulk fluid redistribution among the various tissue compartments, frequently are impacted by disease or trauma. As an example, a common breast cancer phenotype is derangements in hemodynamic states accompanied by increased tissue stiffness and local edema [1]. Accordingly, we have hypothesized that externally applied mechanical forces can produce dynamic responses that are markedly different in diseased and healthy tissues, thereby enhancing diagnostic image contrast. Evidence for this sort of contrast-enhancing effect comes from our previously observed correspondences between fNIRS-based hemodynamic image data and results of computed estimates of internal mechanical stress and pressure distributions [2]—which suggest that spatial distributions of hemodynamic variables in the fNIRS images represent redistributions of blood in response to changes in internal stresses—and from similar imaging-with-compression studies carried out elsewhere [3].

2. Methods

To evaluate the hypothesis that controlled articulations can image contrast between breast tumors and surrounding healthy tissue, we conducted a pre-clinical study using an fNIRS-based breast imaging system whose design criteria included the ability to perform applied-pressure maneuvers [4]. After research participants gave informed consent and provided a brief medical history, they were seated and the sensing heads, which contain the articulating elements used to execute the pressure maneuvers (Figure 1) and monitor the resulting skin displacements (Figure 2), were adjusted to make good contact with both breasts. Following a five-minute baseline scan, the skin-optode contact pressure was rapidly (~2 s) increased to a level of either 4.4 N or 7.1 N, and data collection continued during the subsequent period of stress relaxation (60-120 s).

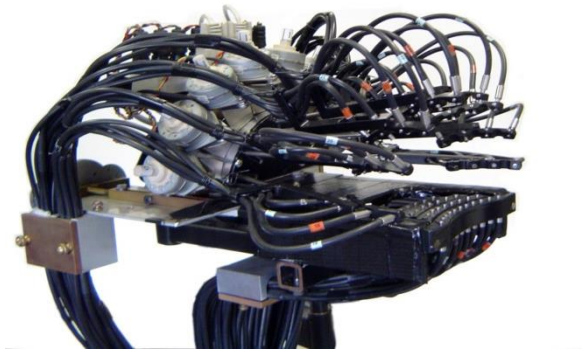

Figure 1. A photograph of one of the left-breast sensing head. The right-breast sensing head is a mirror image of the one shown.

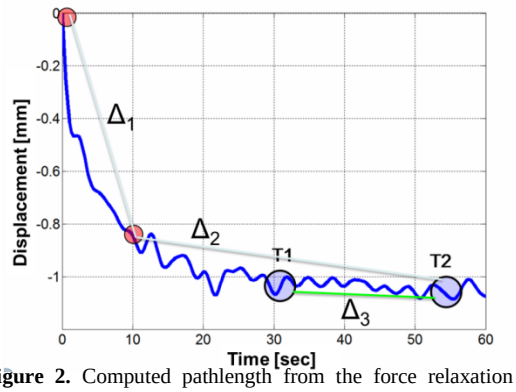

Figure 2. Computed pathlength from the force relaxation after a 7.1 N full compression. Subject was 43 year old, BMI of 35, and with size D breast.

Optical data were analyzed offline: application of a low-pass filter with a 0.2-Hz cutoff frequency was followed by use of the Normalized Difference Method to reconstruct images of oxygenated and deoxygenated hemoglobin (HbO, HbD), tissue oxygen saturation (HbSat), and blood volume (HbT) [5]. Data used for image reconstruction were

limited to measurement time frames after the cessation of significant tissue displacement (Figure 2), to eliminate possible confounds between hemoglobin concentration changes and optical pathlength changes.

A statistical binning technique was applied in order to enhance the contrast between tumor tissue and healthy tissue in the reconstructed images. The essence of the method is that hemodynamic parameter values in every image voxel are replaced with a dimensionless measure of the statistical difference between that voxel and the average across the entire breast. For analyses involving a single hemodynamic parameter, the statistical-difference measure used was the z-score. When two parameters were considered simultaneously, in order to take advantage of their inter-correlations, the Mahalanobis distance was used [6]. In either case, the contrast between tumor and non-tumor tissues was further enhanced by referencing image values for one breast to the image mean and (co)variance of the other, as indicated in Eq. (1).

$$Z_{\text{breast1}} = \frac{x_{\text{breast1}} - \bar{x}_{\text{breast2}}}{s^2_{\text{breast2}}}, \quad MD_{\text{breast1}} = \sqrt{\left(\mathbf{x}_{\text{breast1}} - \bar{\mathbf{x}}_{\text{breast2}}\right)^{\mathrm{T}} \mathbf{C}^{-1}_{\text{breast2}} \left(\mathbf{x}_{\text{breast1}} - \bar{\mathbf{x}}_{\text{breast2}}\right)}, \tag{1}$$

where x is a selected hemodynamic parameter, and $\mathbf{x}$ is a vector of two parameters; $\bar{x}$ and $\bar{\mathbf{x}}$ are the spatial mean averages of x and $\mathbf{x}$, respectively; s^2 is the spatial variance of x, and $\mathbf{C}$ is the spatial covariance matrix for $\mathbf{x}$.

3. Results

Imaging results obtained from 61 subjects (17 breast cancer, 21 benign pathology, 23 healthy control) are consistent with the hypothesis that the articulation maneuvers enhance the contrast between tumor and healthy tissue. Also noteworthy is the finding that image contrast is improved by transforming pairs of co-varying image-values [i.e., (HbD,HbSat), (HbD,HbT), or (HbSat,HbT)] to measures of the statistical extremeness (i.e., the Mahalanobis distance) for each image voxel, as illustrated in Figure 3. The magnitude of the preceding effect is maximized by referencing the image-pixel data of one breast to the distribution of image values for the contralateral breast. At the group level, the paired difference between the numbers of image pixels identified as abnormal is greater for subjects with breast cancer than for either of the other sub-groups, by a statistically highly significant amount ($p \leq 0.007$, unequal variance t-test). In addition, diagnostic accuracies for breast cancer of 90% (ROC analysis [7]) can be achieved, as shown in Table 1.

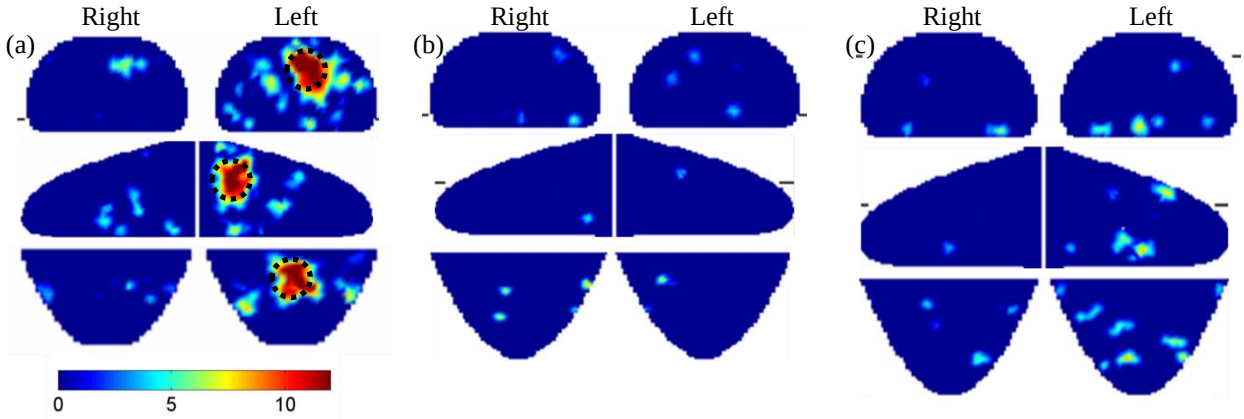

Figure 3. Orthogonal 2D sections (top to bottom: coronal, sagittal and axial) of 3D spatial maps of the MD calculated using Eq. (1). To emphasize large-MD features, images are thresholded to show only regions with MD > 5.5. While similar results are obtained for all pairings of Hb-signal components, the images shown are MDs derived from the (HbT,HbD) pair, from data collected during stress relaxation following a 4.4-N mediolateral compression. (a) Subject with breast cancer: 50 y/o, size D breasts, BMI = 44, and a 4-cm invasive ductal carcinoma in the left breast. Black dotted circles indicate that the tumor size and location, as determined from surgical and conventional imaging procedures, closely agree with the regions of highest MD values. (b) Subject with non-cancer breast pathology: 67 y/o, size D breasts, BMI = 30, and a 4-cm fibroadenoma in the right breast. (c) Healthy-control subject: 58 y/o, size D breasts, BMI = 31.

4. Discussion

The study and analysis presented demonstrate that controlled manipulation of the force applied to the breast tissue can enhance the detectability of cancer, by exploiting a known tumor phenotype. The impact of pressure maneuvers on reconstructed images is maximized when the image-voxel data of one breast are referenced to the distribution of image values for the contralateral breast. Among other things, this demonstrates the utility of the simultaneous dual-breast measurement approach. Of the fNIRS-based breast imagers reported to date, to our knowledge this strategy

has been implemented only in the instrument described in [4]. Also noteworthy is the finding that the highest diagnostic accuracy was achieved from data obtained under a mild compression protocol, involving the lower final pressure value and activation of only half of the articulating elements. This is an illustration of an instrumental design that allows for fine control over the amount of force applied, and of the percentage and which aspect of the breast surface (e.g., medial and lateral vs. top and bottom surfaces) it is applied to.

Table 1. ROC analysis results for paired differences between the number of pixels that have MD larger than 5.5 in each breast. ML/Full = mediolateral/all articulating elements (Fig. 1) are used to apply pressure; 4.4/7.1 = the magnitude of the force applied by each articulating element; Comp/Relax = data collected while tissue responds to the application/release of external force.

Compression Protocol	AUC (%)	Std. Error	Asymptotic Significance	AUC 95% Confidence Interval	
4.4N_Full_Comp	82.4	6.7	< 0.001	69.4	95.5
4.4N_ML_Relax	89.8	4.4	< 0.001	81.1	98.5
7.1N_Full_Comp	78.7	6.3	0.001	66.4	91.0
7.1N_ML_Relax	82.1	5.9	< 0.001	70.5	93.6
7.1N_ML_Comp	78.1	7.0	0.001	64.4	91.8

5. Acknowledgements
This research was supported by the National Institutes of Health (NIH) grant R41CA096102, the U.S. Army grant DAMD017-03-C-0018, the Susan G. Komen Foundation, the New York State Department of Health (Empire Clinical Research Investigator Program), the New York State Foundation for Science, Technology and Innovation–Technology Transfer Incentive Program (NYSTAR-TIPP) grant C020041, and NIRx Medical Technologies.

6. References

[1] P. Vaupel, in *Tumor Blood Flow* (Springer, 2000), 41-45.

[2] R. Al abdi, G. Feuer, H.L. Graber, S. Saha, and R.L. Barbour, "Optomechanical Imaging: Biomechanic and Hemodynamic Responses of the Breast to Controlled Articulation," Poster BSu3A.92 at Biomedical Optics and Digital Holography and Three-Dimensional Imaging (Miami, FL, April 29 - May 2, 2012).

[3] S.A. Carp, A.Y. Sajjadi, C.M. Wanyo, Q. Fian, M.C. Specht, L. Schapira, B. Moy, A. Bardia, D.A. Boas, and S.J. Isakoff, "Hemodynamic signature of breast cancer under fractional mammographic compression using a dynamic diffuse optical tomography system," Biomedical Optics Express **4**, 2911-2924 (2013).

[4] R. Al abdi, H.L. Graber, Y. Xu, and R.L. Barbour, "Optomechanical imaging system for breast cancer detection," J. Optical Society of America A **28**, 2473-2493 (2011).

[5] Y. Pei, H.L. Graber, and R.L. Barbour, "Influence of systematic errors in reference states on image quality and on stability of derived information for DC optical imaging," Applied Optics **40**, 5755-5769 (2001).

[6] R. De Maesschalck, D. Jouan-Rimbaud, and D.L. Massart, "The Mahalanobis distance," Chemometrics and Intelligent Laboratory Systems **50**, 1-18 (2000).

[7] C.E. Metz, "Basic principles of ROC analysis," Seminars in Nuclear Medicine **8**, 283-298 (1978).